

# Cross Ambiguity Function Computation Using Over-Sampled DFT Filter Banks

KENNETH P. BENTZ  
The Aerospace Corporation  
15049 Conference Center Dr.  
Chantilly, VA, USA 90245-4691

*Abstract:* - This paper will demonstrate a new method to compute the Cross Ambiguity Function (CAF) using over-sampled Perfect Reconstruction Discrete Fourier Transform (DFT) filter Banks, and compare it to previous work with maximally decimated DFT Filter Banks [1]. As was shown in our previous work, the DFT Filter Bank can be used to efficiently filter the signal into sub-bands, compute the CAF in each sub-band, and then reconstruct the CAFs coherently. This method has the advantage that Narrow Band (NB) interference can be removed prior to the reconstruction. If the prototype filter satisfies specific conditions, the CAF can be reconstructed coherently, thereby improving the Time Difference of Arrival (TDOA) estimate while maintaining the Frequency Difference of Arrival (FDOA) estimate.

Maximally decimated Filter Banks are most efficient from a computational viewpoint, but the choice of the prototype filter is limited to a very simple filter with poor (13 dB) side-lobes. The over-sampled DFT filter bank is somewhat more computationally complex, but filters can be designed with better side-lobe properties, so that interference can be removed more efficiently. The prototype filter for the over-sampled filter bank can be designed with lower side-lobes, which removes more of the interferer and less of the signal of interest. The design constraints for the prototype filter for the over-sampled filter bank are the same as that of the cosine modulated filter bank.

*Key-Words:* - Cross Ambiguity Function, DFT Filter Bank, Perfect Reconstruction Filter Bank.

## 1 Introduction

### 1.1 Use of CAF to estimate TDOA and FDOA

The CAF is used in signal processing to estimate the TDOA and FDOA of a signal received at two spatially separated receivers. The TDOA/FDOA estimates can then be used to estimate the location of the transmission source relative to the receivers. The output Signal to Noise Ratio (SNR) of the CAF improves proportionally to the Time-Bandwidth product of the signal. The estimate of the TDOA and FDOA occurs at the CAF peak. When the Time-Bandwidth product is much less than one, the following formula can be used to compute the CAF.

$$CAF(\tau, f) = \int_{-\infty}^{\infty} r_1(t) \overline{r_0(t-\tau)} e^{-j2\pi ft} dt \quad (1)$$

where  $r_1(t)$  and  $r_0(t)$  are the low pass equivalent signals. Computation over all possible delay and frequency bins would be computationally intensive, but since in many applications the FDOA is much smaller than the sampling rate, the search range can be significantly reduced. This can be accomplished by using a Low Pass Filter (LPF) and then down-sampling. A computationally efficient mechanism is

a simple integrate and dump, which greatly simplifies the computational complexity, at the expense of a filter with poor stop-band characteristics. Zero-padding the output of the down-sampler is used to get the proper doppler bin spacing. Figure 1 shows a block diagram of a typical CAF processor.

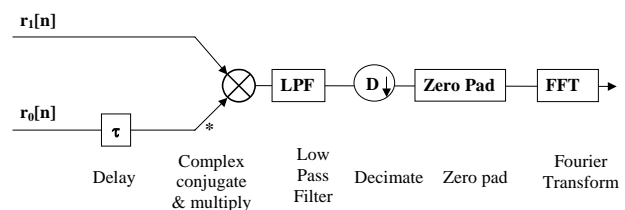


Figure 1. Typical CAF processor

The CAF is an efficient estimator since it is unbiased, and achieves the Cramer-Rao Lower Bound (CRLB).<sup>2</sup> The standard deviation of the TDOA and FDOA estimates are proportional to the inverse of the square root of the BTγ product, where B is the signal bandwidth, T is the integration time, and γ is the input SNR.

$$\sigma_{TDOA} \propto \frac{1}{\sqrt{BT\gamma}}, \text{ and } \sigma_{FDOA} \propto \frac{1}{\sqrt{BT\gamma}} \quad (2)$$

Figure 2 shows an example of a CAF of a Minimum Shift Keying (MSK) signal at 0 dB input SNR with the TDOA and FDOA equal to zero.

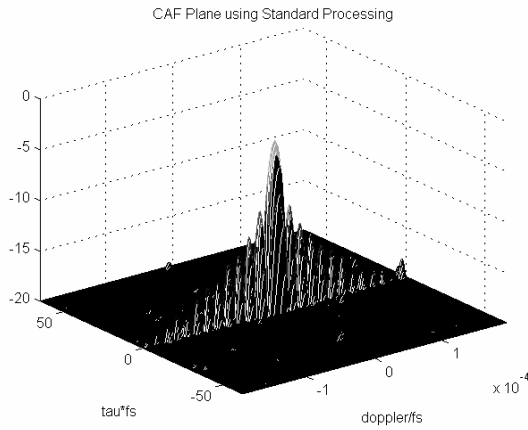


Figure 2. CAF of MSK signal at 0 dB input SNR

### 1.2 Effect of NB Interference on CAF plane

Computing the CAF of a Wide-Band (WB) signal in the presence of narrowband interference can significantly degrade the TDOA and FDOA estimates, because the main lobe of the narrowband signal is much wider than the WB signal, and can therefore obscure the true TDOA/FDOA of the WB signal. Figure 3 is an example of two MSK signals of equal power, but different bandwidths.

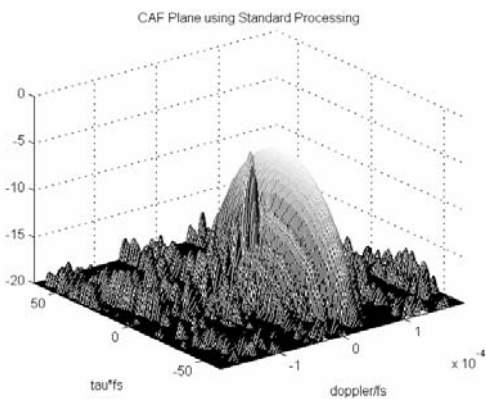


Figure 3. CAF with WB signal and NB interferer

### 1.3 Performance Impact of Non-coherent Processing

As suggested by Stein in [3], one way to work around this problem is to filter the signal into sub-bands, eliminate the interference, and then recombine the results. The problem with this is that recombining the results non-coherently degrades the

variance of the TDOA estimate by a factor equal to the number of sub-bands. Figure 4 shows the same case as above, but with the signal filtered into M=16 sub-bands, the interference removed, and then added non-coherently. From the figure, it is clear that the TDOA estimate is significantly degraded. In fact, as predicted, the variance has degraded by a factor of M=16, and the standard deviation by a factor of 4.

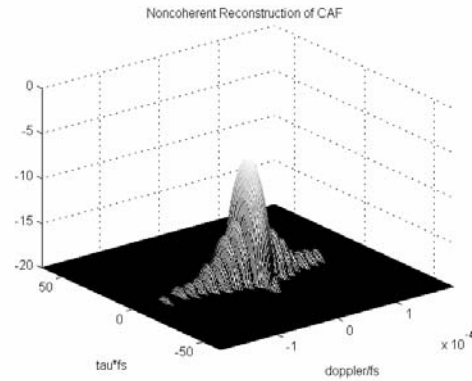


Figure 4. CAF after non-coherent reconstruction

## 2 Problem Formulation

### 2.1 CAF Processing using DFT Filter Bank

Vaidyanathan<sup>3</sup> proposed a method for performing convolution in sub-bands using Perfect Reconstruction Filter Banks (PRFBs) as in fig 5. Since convolution and correlation are mathematically similar (i.e. the convolution of  $r_0[n]$  and  $r_1^*[-n]$  is equivalent to the correlation of  $r_0[n]$  and  $r_1[n]$ ), his method can also be used for correlation. His motivation was to show how his method could be used to obtain a coding gain over direct convolution by basing the sub-band quantization on signal power. Sufficient conditions for perfect reconstruction are that the filters satisfy (3), where K is the decimation ratio, M is the number of sub-bands, and M/K is an integer. For maximally decimated filter banks,  $K=M$ .

$$\frac{1}{M} \sum_{m=0}^{M-1} H_m(W_K^k z) \overline{H_m(z^{-1})} = \delta(k) \text{ for } k = 0, 1, \dots, K-1 \quad (3)$$

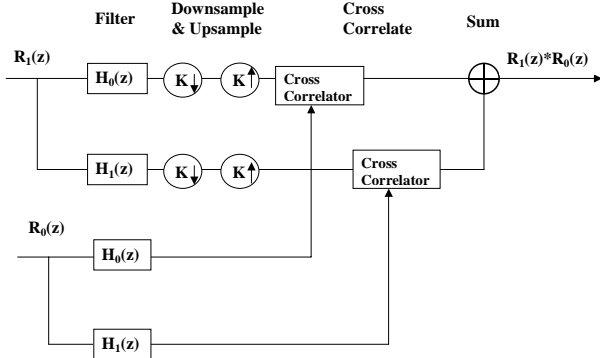


Figure 5. Implementation of sub-band convolver

The architecture in figure 5 increases the processing burden by a factor of M, since there are now M correlations, each of length of the original input sequence. The filtering and decimation/expansion steps can be greatly simplified by using the polyphase implementation. The correlation step can also be greatly reduced by noticing that, after up-sampling  $r_1[n]$ ,  $(M-1)/M$  of the samples contains zeros, so many of the operations are unnecessary. This can be corrected by taking the output of  $r_0[n]$  from the DFT filter bank, delaying the signal K times, and down-sampling by a factor of K. We now have to calculate  $M*K$  correlations, but each is at the decimated rate. The corresponding realization for the CAF processing is shown in Fig 6.

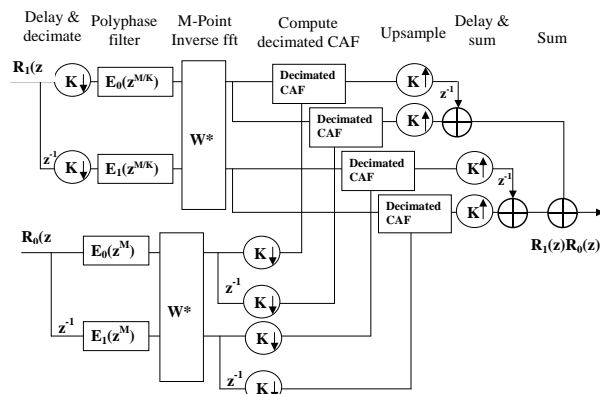


Figure 6. Efficient implementation of CAF with Perfect Reconstruction DFT Filter Bank

### 3 Problem Solution

#### 3.1 Maximally Decimated DFT Filter Banks

In the above example, if  $K=M$ , the filter bank is maximally decimated. Maximally decimated DFT filter banks are very efficient. One major issue, though, is that the only filters which satisfy the perfect reconstruction criteria of (3) are filters with exactly M non-zero coefficients where each of their coefficients are of equal magnitude, as the filter in

(4). In this case, the filters each have 13 dB side-lobes. This may not be acceptable if the NB interference is sufficiently strong. The advantage is that the structure is simplified, since each polyphase component is equal to unity, and the polyphase filter step of Figure 6 can be omitted.

$$P(z) = \frac{1}{\sqrt{M}} \left( 1 + z^{-1} + \dots + z^{-(M-1)} \right) \quad (4)$$

#### 3.2 Over-sampled DFT Filter Bank

A slightly less efficient, but more flexible structure is implemented with an over-sampled filter bank. If the decimation ratio, K is equal to half the number of sub-bands, then the prototype filter can be designed with less constraints and better side-lobe performance.

In general, nonlinear optimization techniques are required to find filters that meet the necessary criteria of (3). Several methods for creating the prototype filters can be found in [4] and [5]. For prototype filters of length  $N=2M$ , a simple closed-form expression for the zero-phase prototype filter as given in (5) can be used.<sup>6</sup> Figure 7 compares the frequency response of the filters represented in (4) and (5) for  $M=16$ .

$$p(n) = \frac{1}{\sqrt{2M}} \cos \left( \pi \left( \frac{n}{M} + 1 \right) \right) - \frac{1}{\sqrt{4M}} \text{ for } n = -\frac{(N-1)}{2}, \dots, \frac{(N-1)}{2} \quad (5)$$

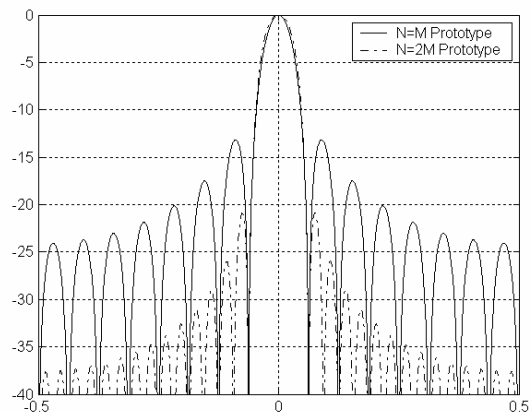


Figure 7. Frequency Response of prototype filters with length  $N=M$  and  $N=2M$

#### 3.3 Assessment of Computational Complexity

Assume that  $N_t$  is the number of samples of the Low Pass Equivalent (LPE) signal,  $N_r$  is the number of delay values of interest, and  $N_\omega$  is the number of doppler values of interest. For each delay value of interest, we must multiply each sample of  $r_0$  with the

complex conjugate of  $r_1$  delayed by  $\tau$ , filter, decimate, and perform an FFT. The number of complex multiplications is then  $N_\tau \cdot (N_\tau + N_\omega \cdot \log_2(N_\omega))$

For the DFT filter bank architecture, we must first filter the signals into sub-bands. Assume  $L$  equals the length of the prototype filter,  $M$  is the number of sub-bands, and  $K$  is the decimation ratio (either  $M$  or  $M/2$ ). For each input time sample, the first signal requires  $L/K + M/K \cdot \log_2(M)$  complex multiplies, and the second signal requires  $L + M \cdot \log_2(M)$ , for a subtotal of  $(1 + 1/K)(L + M \cdot \log_2(M)) \cdot N_t$ . For the case when  $M = K$ , the polyphase filter step can be skipped, and the subtotal is  $(1 + 1/K)(M \cdot \log_2(M)) \cdot N_t$ .

We must now compute  $M \cdot K$  CAFs, but each is at the decimated rate, so the subtotal is  $N_\tau \cdot (N_\tau \cdot M/K + N_\omega \cdot \log_2(N_\omega))$ . For the case when  $M = K$ , this is identical to the conventional CAF, so the overhead for performing the DFT filter bank is the only additional cost. The total is then  $(1 + 1/K)(M \cdot \log_2(M)) \cdot N_t + N_\tau \cdot N_t \cdot M/K$ . When  $K = M/2$ , we have approximately doubled our computational complexity over that of the maximally decimated filter bank.

Since the filter bank is done once, independent of the number of delay values of interest, the maximally decimated filter bank's computational complexity approaches that of the conventional CAF as the number of delay values of interest increases. The over-sampled filter bank requires approximately twice the number of complex multiplications as the maximally decimated filter bank, independent of the number of delay values of interest.

To further reduce computational complexity, we could compute one decimated CAF in each sub-band first to determine if a signal is present before attempting to process the entire sub-band CAF. This would reduce the computational complexity by  $1/K$  for each band that does not contain the signal.

### 3.4 Simulation Results

#### 3.4.1 Comparison of Conventional Method to PRFB Method

Using the proposed method, a CAF is produced for each sub-band. Figure 8 shows the CAF produced by coherently adding these results. Figure 9 shows a comparison of the two methods by differencing the results of the conventional CAF (Figure 2) with the PRFB method (Figure 8). At zero doppler, the results are identical to within numerical round-off error. A small error occurs for non-zero doppler,

since the doppler correction is essentially applied after the filter bank, rather than prior to the filter bank. This error is small in comparison to the distortion from the low pass filter, and has negligible impact on the TDOA and FDOA estimates.

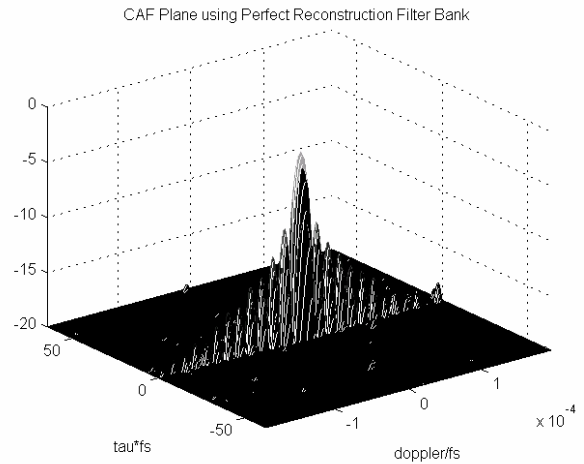


Figure 8. CAF reconstructed from DFT filter bank

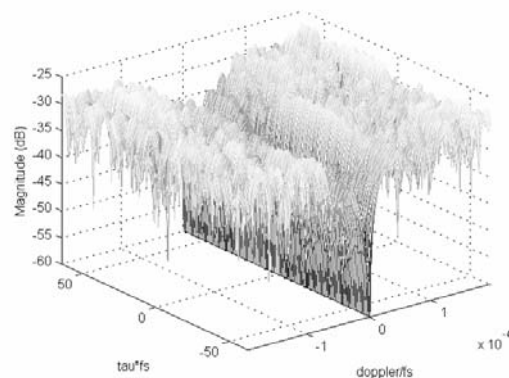


Figure 9. Difference between CAFs computed from conventional method and using filter bank

#### 3.4.2 Comparison of Over-sampled to Maximally Decimated Filter Banks.

Figures 10 and 11 compare the CAFs computed using the maximally decimated filter bank, and the over sampled DFT filter bank after removal of the bands with most of the NB energy. Figure 10 shows that a significant amount of the NB interference was not removed with the maximally decimated filter bank, due to the filter's side-lobe performance. Figure 11 shows the same case, with a prototype filter of length  $2M$ . A significant improvement in removing the NB interference can be seen.

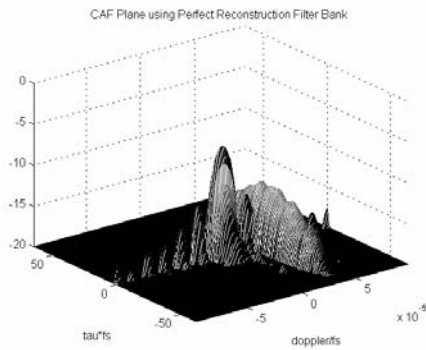


Figure 10. CAF after NB interference removal with prototype of length  $N=M$

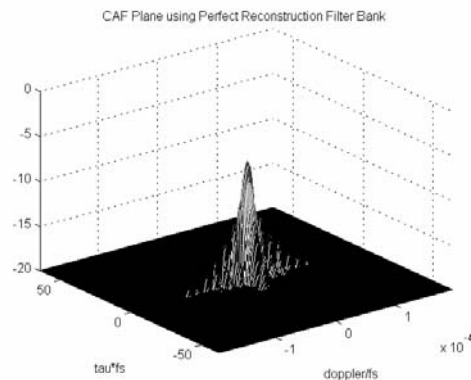


Figure 11 CAF after NB interference removal with prototype of length  $N=2M$

#### 4. Conclusion

An algorithm for computing the CAF with over-sampled DFT Filter Banks was developed, and compared to the conventional CAF processing, and to the maximally decimated CAF previously developed. The performance advantage over conventional CAF processing for removing NB interference was quantified and demonstrated. Maximally decimated PRFB DFT filter banks can be used, but poor side-lobe performance results. Side-lobe performance of over sampled DFT filter banks was significantly better than the maximally decimated DFT filter banks, and hence, more of the NB interferer's energy can be removed.

The same prototype filters can be used for the over-sampled filter bank as is used for Cosine Modulated PRFB prototype filters. It increased the computational complexity over standard CAF processing by approximately two-fold. In practice, however, this could be reduced by selectively processing each of the  $M \cdot K$  decimated CAFs. The architecture also lends itself to be more easily computed in a parallel fashion.

#### References:

- [1] K.P. Bentz, A. Baraniecki, Coherent Cross Ambiguity Function Processing Using Perfect Reconstruction Filter Banks, *Proceedings of the 6<sup>th</sup> IASTED International Conference on Signal and Image Processing, 2004*, pp. 381-384.
- [2] S. Stein, Algorithms for ambiguity function processing, *IEEE Transactions on Acoustics Speech, and Signal Processing*, Vol. 29, No. 3, 1981, pp. 588-599.
- [3] P.P. Vaidyanathan, Orthonormal and biorthonormal filter banks as convolvers, and convolutional coding gain, *IEEE Transactions On Signal Processing*, Vol. 41, No. 6, 1993, pp. 2110-2130.
- [4] R.D. Koipillai, P.P. Vaidyanathan, Cosine Modulated FIR Filter Banks Satisfying Perfect Reconstruction, *IEEE Transactions on Signal Processing*, Vol. 40, No. 4, Apr 1992, pp. 770-783.
- [5] T. Saramaki, R. Bregovic, An efficient approach for designing nearly perfect-reconstruction cosine-modulated and modified DFT filter banks, *Proceedings of 2001 IEEE International Conference on Acoustics, Speech, and Signal Processing (ICASSP '01)*, Volume 6, 7-11 May 2001 pp. 3617 – 3620.
- [6] T. Karp, N.J. Fliege, Modified DFT Filter Banks with Perfect Reconstruction, *IEEE Transactions on Circuits and Systems-II: Analog and Digital Signal Processing*, Vol. 46, No. 11, Nov 1999, pp. 1404-1414.